

Conformational Effects on High-Spin Organic Molecules¹

Scott K. Silverman and Dennis A. Dougherty*

Arnold and Mabel Beckman Laboratories of Chemical Synthesis,[†] California Institute of Technology, Pasadena, California 91125

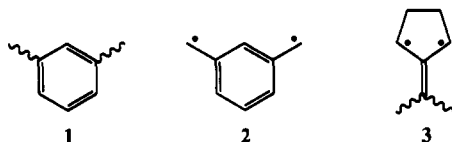
Received: July 19, 1993*

The ability of *m*-phenylene to ferromagnetically couple spin-containing substituents that are substantially twisted out of conjugation is investigated. The “bis(TMM)” strategy is employed, in which two triplet TMM biradicals are linked through *m*-phenylene to produce relatively stable, organic tetradicals that are characterized by EPR spectroscopy. Under conditions of moderate twisting (4), ferromagnetic coupling is seen, and the tetradical has a quintet ground state. Severely twisting both TMMs as in 13 disrupts spin communication, and two noninteracting triplets are produced. This is in contrast to other highly twisted *m*-phenylene derivatives, in which antiferromagnetic coupling has been observed. Surprisingly, severely twisting only one TMM (14) still produces ferromagnetic coupling and a quintet ground state through a spin polarization mechanism analogous to that proposed for 90° twisted ethylene. Several ring-constrained TMMs (17–19) are investigated as models for more nearly planar systems.

Introduction

The rational design and preparation of molecular-based magnetic materials present substantial intellectual and technical challenges and define a major goal of modern organic chemistry.² Of many strategies currently being pursued, we have found the paradigm of Figure 1 to be especially useful.^{3,4} Conceptually, we design a material from two building blocks—the spin-containing unit (SC) and the ferromagnetic coupling unit (FC). The SC is simply any structure that contains a local magnetic moment, such as a radical, radical ion, or transition metal. The FC is a general structural unit linking two (or more) spin-containing units such that they are ferromagnetically (high-spin) coupled rather than antiferromagnetically (low-spin) coupled. We and others have devoted considerable effort into developing and characterizing FCs as a key to the rational design of new magnetic materials.

By far the most studied and best characterized FC is *m*-phenylene (1). It has been shown to ferromagnetically couple many types of radicals, carbenes, and radical ions and remains the best candidate for designing truly magnetic materials.^{3a,e,5} The prototypical structure is *m*-xylylene (2), and a number of studies have provided a convincing rationalization for the high-spin, triplet ground state of this planar, alternant hydrocarbon biradical.⁶ However, real materials designed to display cooperative magnetic behaviors will be structurally more complicated than 2. Deviation from planarity will almost certainly occur, and this could impact the effectiveness of *m*-phenylene as an FC.

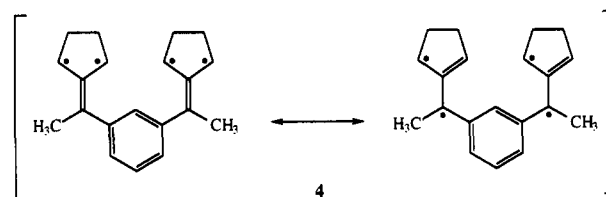


In the present work, we describe studies intended to probe the response of *m*-phenylene to substantial conformational changes involving twisting the SC out of conjugation with the FC. We use the “bis(TMM)” approach that we have recently developed.⁴ This is a general strategy for evaluating FCs qualitatively and, in favorable cases, quantitatively. The method uses a simple trimethylenemethane (TMM) derivative,⁷ 3, as the SC. This structure has several useful characteristics, including strong

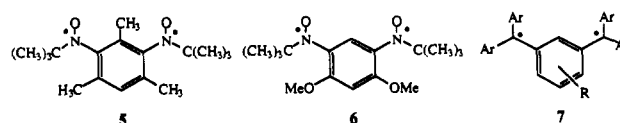


Figure 1. Schematic for design of high-spin molecules and materials. The SC is shown as an arrow.

intrinsic triplet preference, well-characterized EPR spectra, and relatively facile synthetic access by photolysis of appropriate diazene precursors. The prototype bis(TMM) is tetradical 4, which links two TMMs through the *m*-phenylene FC. In previous work⁴ we have shown that 4 has a quintet (Q) ground state.

Effect of Nonplanarity (Twisting) on *m*-Phenylene as an FC

Theoretical studies of 2 have focused on the planar structure, (0,0)*m*-phenylene, as is appropriate for such a simple molecule. However, one expects that twisting the radical centers out of conjugation with the aromatic ring would substantially alter the effectiveness of the FC. Recently, several groups have addressed this issue. In the highly crowded bisnitroxyls 5⁸ and 6,⁹ the two spin-containing units are twisted essentially completely out of conjugation, and the biradicals have *singlet* ground states. This suggests that (90,90)*m*-phenylene is an antiFC. In contrast, several extremely congested polyaryl derivatives (7) of 2 still show high-spin ground states, despite what must be very substantial amounts of twisting.¹⁰



Concerning the present systems, computations (see Experimental Section) suggest that even the parent 4 is significantly twisted out of planarity. To investigate this, we prepared the fulvene 8 and determined its X-ray crystal structure. This fulvene shows significant twisting in the crystal, with $\phi \sim 37^\circ$, suggesting

[†] Contribution No. 8825.

* Abstract published in *Advance ACS Abstracts*, November 15, 1993.

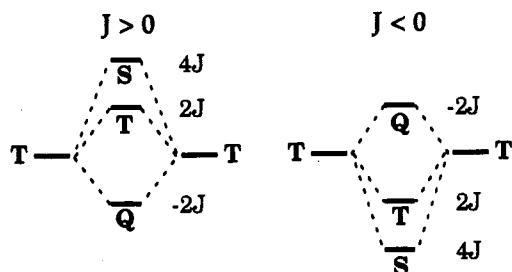


Figure 2. Heisenberg energy level diagrams for the interaction of two triplets described by a single exchange parameter J .

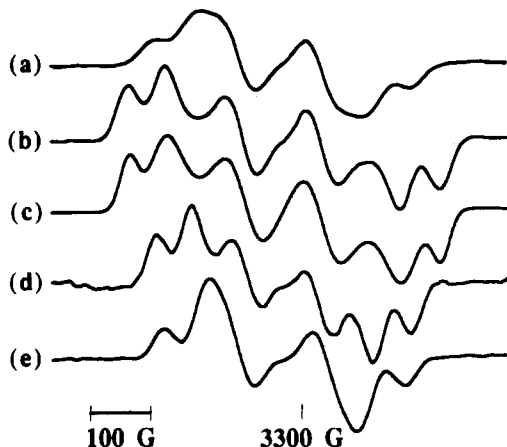
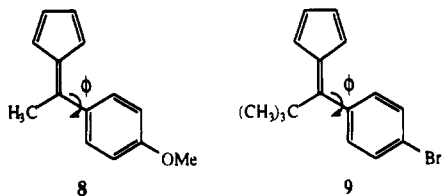


Figure 3. The $\Delta m_s = 1$ region of the EPR spectra observed after photolysis of diazenes at 77 K in MTHF: (a) 10; (b) 11; (d) 17; (e) 18; (c) simulation of the spectrum in (b) with zfs parameters from Table I.

that the quintet preference in 4 may be less than in our previous prediction⁴ based on a planar structure.



When two triplets are linked through a potential FC, one can expect one of the two state orderings of Figure 2, depending on whether ferromagnetic coupling ($J > 0$) or antiferromagnetic coupling ($J < 0$) occurs.⁴ This is simply the well-known result of applying a standard Heisenberg Hamiltonian to a T + T coupling. Previously, we predicted⁴ a Q-T gap of 2200 cal/mol for planar 4, based on the calculated S-T gap in 2 and arguments concerning spin density at the carbons attached to the benzene ring. Assuming ferromagnetic coupling scales with orbital overlap, and thus $\cos \phi$, the expected Q-T gap is $\cos(37^\circ) \times \cos(37^\circ) \times 2200 = 1400$ cal/mol, still consistent with our experimental estimate⁴ of a gap > 1300 cal/mol.

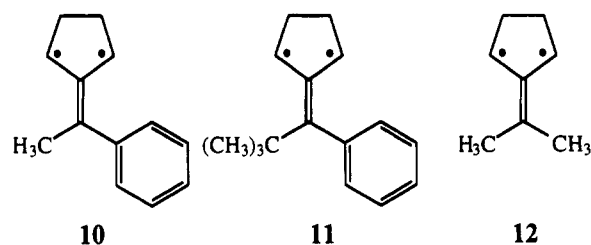
Our structural calculations also suggest that replacing the methyl groups of 4 with *tert*-butyl groups would completely twist the *m*-phenylene ring out of conjugation with the TMMs. This is supported by the X-ray crystal structure of 9, which shows the phenyl and fulvene planes nearly perpendicular ($\phi \sim 87^\circ$). For further corroboration, we compared the EPR zero-field splitting (zfs) D values (Figure 3, Table I) for TMMs 10 and 11 (prepared by photolysis of standard diazene precursors). Since D is a sensitive probe of the average interelectron separation in a triplet, it is a good indicator of the extent to which the phenyl rings of 10 and 11 delocalize the TMM spins.¹¹ As expected, the D value for 11 is greater than that for 10 (Table I). In fact, $D(11)$ is nearly equal to that for the dimethyl compound 12 (Table I),

TABLE I: Zero-Field Splitting Parameters for Triplet TMMs

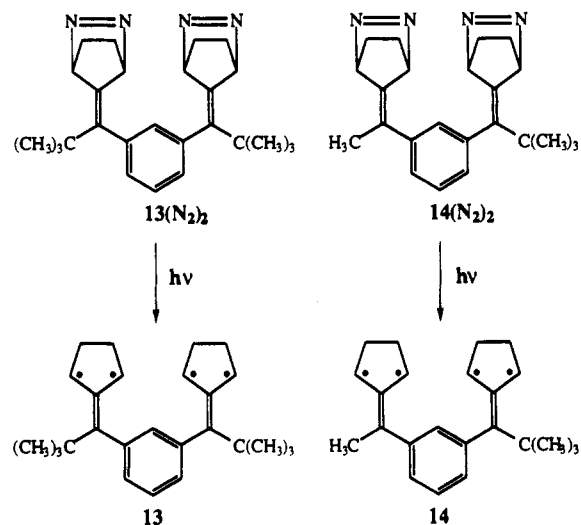
TMM	$ D/hc , \text{cm}^{-1}$ ^a	$ E/hc , \text{cm}^{-1}$ ^a
10	0.0195 ^b	0.001 75 ^b
11	0.0241	0.004 06
12	0.0256 ^c	0.003 4 ^c
17	0.0196	0.002 70
18	0.0186	0.001 28
19	0.0169 ^b	0.001 60 ^b

^a Determined from the EPR spectra observed after photolysis of the corresponding diazene at 77 K in MTHF. All spectra are well simulated using standard methods.⁴ ^b These biradicals display temperature-dependent behavior; see text for details. ^c Platz, M. S.; McBride, J. M.; Little, R. D.; Harrison, J. J.; Shaw, A.; Potter, S. E.; Berson, J. A. *J. Am. Chem. Soc.* 1976, 98, 5725-5726.

confirming a negligible amount of phenyl delocalization in 11.



The *tert*-butyl-substituted analog of 4 is bis(TMM) 13. The FC is no longer planar *m*-phenylene but instead a doubly twisted (90,90)*m*-phenylene. If the TMMs are perpendicular to the phenyl ring, then little unpaired spin density would reside on the phenyl ring, and one expects little spin communication between the TMM subunits.



Photolysis of the bisdiazene 13(N_2)₂ gives rise to a triplet TMM EPR signal *identical* to that of 11. The $\Delta m_s = 1$ signal consistently grows in with first-order kinetics, and the spectral shape remains the same even after prolonged photolysis and cooling to 4.4 K. The $\Delta m_s = 2$ region is also identical to that of 11, and a Curie plot of its intensity is linear from 10 to 70 K. We have a great deal of experience with the bis(TMM) approach,^{4,12} and we are confident that under these conditions a significant number of precursor molecules have had both N_2 units expelled to produce tetradical 13. We conclude that 13 consists of two noninteracting triplet subunits within the same molecule. One could argue that 13 is simply EPR-silent, because it has a singlet ground state or because it reacts with itself to give a low-spin product.¹³ However, under such circumstances the triplet EPR signal would grow in and then decay on extended photolysis, as we have seen previously in another bis(TMM) molecule built around an

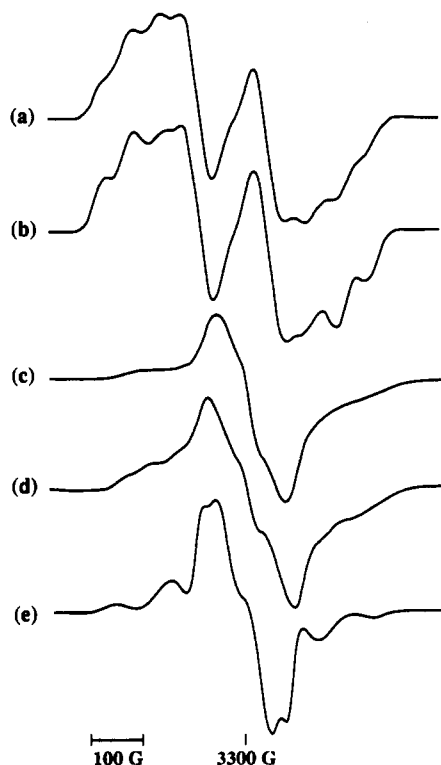


Figure 4. (a) $\Delta m_s = 1$ spectrum observed after brief photolysis (5 min) of $14(N_2)_2$ at 77 K in MTHF. (b) Predicted spectrum obtained by adding the experimental spectra of **10** and **11** (Figure 3a and 3b) in a 1:1 mole ratio. (c) $\Delta m_s = 1$ spectrum observed after photolyzing $14(N_2)_2$ for 9.5 h at 50 K in propylene glycol, annealing at 135 K, and cooling to 11.8 K. (d) Sample in (c) warmed to 135 K. The changes with temperature are reversible. (e) Experimental spectrum of quintet **4** (ref 4).

antiFC.⁴ Thus, in the present context, (90,90)*m*-phenylene is neither an FC nor an antiFC, at least at temperatures ≥ 4.4 K. Instead, it merely insulates two spin-containing units from one another, allowing them to act independently.

This is in sharp contrast to the previously mentioned bisnitroxyls **5** and **6**, in which (90,90)*m*-phenylene acts as an antiFC.^{8,9} While we have no simple rationalization for this dichotomy, we note that nitroxyl is an unusual spin-containing unit, which has a significant spin-orbit coupling term. This may contribute to the behavior seen in **5** and **6**. Another bis(triplet) tetradical has been reported in which an ethylene unit serves as the spacer.¹⁴

If (0,0)*m*-phenylene is a good FC and (90,90)*m*-phenylene is neither an FC nor an antiFC, what is (0,90)*m*-phenylene? The bis(TMM) approach offers a straightforward means of answering this question using tetradical **14**, which contains both a methyl-substituted and a *tert*-butyl-substituted TMM. The bisdiazene $14(N_2)_2$ was prepared. Brief photolysis gives a $\Delta m_s = 1$ signal that clearly arises from a 1:1 mixture of the singly denitrogenated triplet TMM monodiazenes **15** and **16** (Figure 4a,b). Note that the computed spectrum of Figure 4b is not a fitted simulation. Rather, it is a *predicted* spectrum obtained with no adjustments by simply summing the *experimental* spectra for **10** and **11** in a 1:1 ratio. This modularity of design constitutes another advantage of the bis(TMM) approach.

Extended photolysis of $14(N_2)_2$ (Figure 4c,d) leads to a familiar sequence⁴ in which dramatic changes occur, especially in the middle of the spectrum. We assign the final spectrum as due to the quintet state of **14**, based on its strong resemblance to the signal observed for the quintet ground state of **4** (Figure 4e)⁴ and several related structures.¹² At present we consider it likely that the quintet we observe is the ground state of **14**, since the signal is intense at temperatures as low as 4.5 K. We note that these spectra are somewhat featureless, and it is possible that they do not represent pure quintets but contain some contribution from

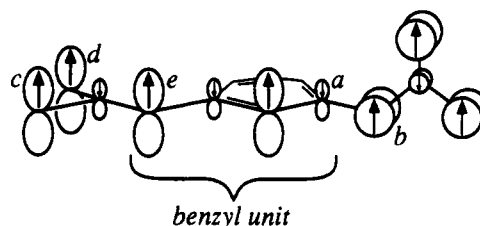
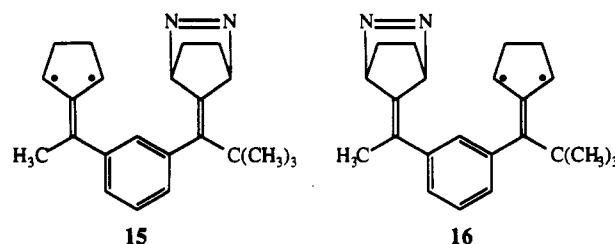


Figure 5. Schematic of the π system of **14**, indicating spin polarization pattern.

the tetradical triplet state. This is especially so given the small Q-T gap expected for the system (see below).



A rationalization for the quintet ground state in **14** can be developed with reference to Figure 5. We view **14** as two orthogonal triplet subunits, one similar to **10** and the other similar to **11**, interacting to produce a quintet state. The delocalized **10**-like TMM communicates with the relatively localized **11**-like TMM through the *a*-*b* bond, a connection that resembles perpendicular D_{2d} ethylene. Calculations predict that twisted ethylene has a singlet ground state due to spin polarization effects.¹⁵ Thus, perpendicular ethylene is an antiFC, but in this case a center of negative spin density (*a*) is antiferromagnetically coupled to one of positive spin density (*b*). This produces a net alignment of the positive spin densities and thus overall ferromagnetic coupling (Figure 5).

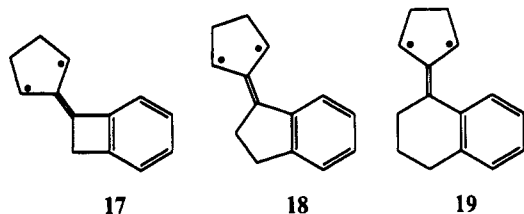
We can use the twisted ethylene model to predict the Q-T gap in **14**. The calculated S-T gap in perpendicular ethylene is ~ 2 kcal/mol,¹⁵ and since the S-T gap in a biradical is $2J$, $J_{eth} \sim -1$ kcal/mol. The J for **14** (J_{14}) is related to J_{eth} in a straightforward way. J_{14} should be positive because the spin densities at the joined carbons *a* and *b* are of opposite sign (Figure 5) and because J_{eth} is negative. To a first approximation, $|J_{14}|$ equals $|J_{eth}|$ scaled appropriately to account for the reduced spin densities at the connecting carbons. As discussed previously,⁴ the scaling factor is $1/3$ for the "out-of-plane" TMM, because only $1/3$ of the TMM total spin density is located at the carbon (*b*) that connects to the FC. The spin density on carbon *a* involves two scaling factors. The total TMM spin density is to first order apportioned as follows: $1/3$ on carbon *c*, $1/3$ on carbon *d*, and $1/3$ on the benzyl unit shown in Figure 5. In benzyl radical, hyperfine coupling constants¹⁶ indicate that the (negative) spin density at the carbon corresponding to *a* is 0.11 of the density at the benzylic center (*e*). Thus, the scaling for center *a* is $1/3 \times 0.11$, and J_{14} equals J_{eth} multiplied by $-1/3 \times 0.11 \times 1/3$, or about $+12$ cal/mol. The predicted Q-T gap is then $4J_{14} \sim 50$ cal/mol. A gap in this range should be accessible at low temperatures, and we note that there are reversible temperature effects in the spectra for **14** (Figure 4c,d). The new peaks growing in at higher temperatures could be consistent with thermal population of a triplet state, but confirmation of this assignment will require further supporting evidence.

These results indicate that (0,90)*m*-phenylene is an FC, although probably a weak one. Structure **14** represents a novel strategy in which a fundamentally antiferromagnetic coupling unit—twisted ethylene—is used to produce overall ferromagnetic coupling by linking sites of oppositely signed spin densities. This

may be a useful strategy, especially with spin-containing units that contain large spin polarizations and thus large negative spin densities.

Constrained Systems

Given the substantial twisting in **11/13** and the nontrivial twisting presumably present in **10/4**, we felt it would be interesting to investigate structures designed to be more nearly planar. This may be valuable for future designs that want to make optimal use of the *m*-phenylene FC. Therefore, we have prepared the constrained-ring TMMs **17**, **18**, and **19**, for comparison to **10** and **11**.



Model calculations (see Experimental Section) on these biradicals and UV data for the analogous fulvenes¹⁷ indicate that **17** is essentially planar, **18** less so, and that **19** and **10** have roughly the same twist. As indicated earlier, **11** likely has the phenyl ring essentially perpendicular to the TMM plane. One complication is that not only may the phenyl ring twist out of the plane of the TMM, but the TMM itself may twist internally, complicating detailed analysis of such structures. To first order, however, based on the simple trend above, we expected the *D* value of **17** to be small, that of **18** somewhat larger, those of **19** and **10** larger still, and that of **11** to be the largest.

The EPR spectra of biradical **17** are straightforward (Figure 3). Photolysis of the diazene precursor at 77 K in MTHF gives a $\Delta m_s = 1$ spectrum with $|D/hc| = 0.0196$, $|E/hc| = 0.00270$ cm⁻¹. The spectrum is unchanged at 3.8 K. The $\Delta m_s = 2$ spectrum (not shown) is a nonet, a_H 12.2 G, due to hyperfine coupling to eight hydrogens, two α and six β .¹⁸ We have previously shown¹⁹ that in such TMMs the magnitudes of the α and β hyperfine splittings are very similar, and pleasingly simple splitting patterns are observed.

The EPR spectra of biradical **18** are also straightforward (Figure 3). Photolysis of the diazene precursor at 77 K in MTHF gives a $\Delta m_s = 1$ spectrum with $|D/hc| = 0.0186$, $|E/hc| = 0.00128$ cm⁻¹. A nearly identical spectrum is observed in propylene glycol. The $\Delta m_s = 2$ spectrum is a nonet, a_H 11.25 G.¹⁸ Photolysis of the diazene at 4.0 K gives the same $\Delta m_s = 1$ and 2 spectra as at 77 K.

We have observed interesting temperature-dependent behavior in biradical **19** (Figure 6). Photolysis of the diazene precursor at 77 K in MTHF gives a $\Delta m_s = 1$ spectrum with $|D/hc| = 0.0169$, $|E/hc| = 0.00160$ cm⁻¹. A nearly identical spectrum is observed in propylene glycol. Photolysis at 4.0 or 50.0 K gives a similar but slightly different spectrum, with $|D/hc| = 0.0165$, $|E/hc| = 0.00214$ cm⁻¹. Warming the sample to 77 K causes the high-temperature spectrum to be irreversibly restored.

Significant temperature effects are also observed in the $\Delta m_s = 2$ region (Figure 7). Photolysis at 77 K gives a nonet, a_H 11.6 G. Photolysis at 4.0 or 50.0 K gives an octet with a_H 11.6 G.¹⁸ Warming the sample to 75.0 K gives the nonet. Thus, the low-temperature spectra indicate hyperfine coupling to only seven hydrogens, but the high-temperature spectra indicate coupling to eight. The octet to nonet conversion is irreversible and occurs at approximately the same temperature as the irreversible changes in the $\Delta m_s = 1$ spectrum. This strongly suggests that all the changes are due to the same process, most likely a conformational change in the TMM after nitrogen loss from the diazene precursor.

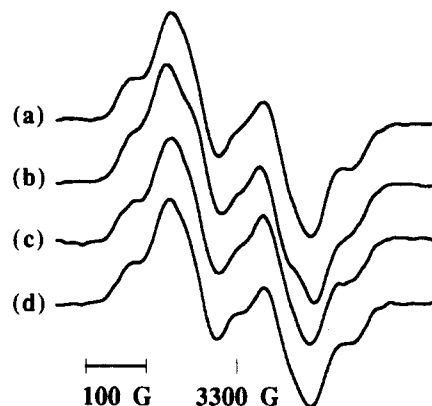


Figure 6. $\Delta m_s = 1$ spectra observed after photolysis of **19**(N₂) in MTHF: (a) photolysis at 77 K in liquid nitrogen, (b) photolysis at 50 K in the cryostat, (c) sample in (b) warmed to 77 K, (d) sample in (b) cooled to 50 K. The changes with temperature are irreversible.

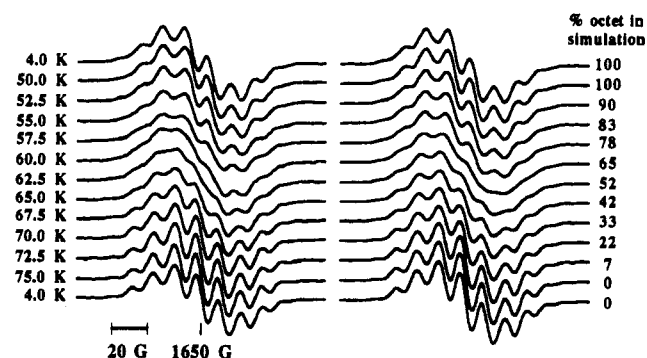
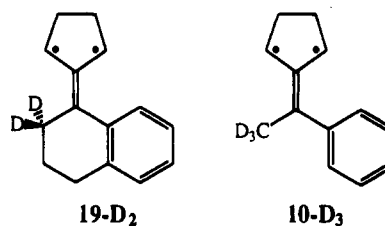


Figure 7. $\Delta m_s = 2$ spectra observed after photolysis of **19**(N₂) at 4.0 K in MTHF. Left side: experimental spectra, slowly increasing the temperature moving down the column. The changes with temperature are irreversible, as the limiting 4.0 K spectra demonstrate. Right side: simulation of the experimental spectra as a weighted sum of the 4.0 K octet (top) and nonet (bottom) spectra. The percent octet used in each simulation is shown on the far right.

The deuterated TMM **19-D₂** was prepared by photolysis of the diazene precursor. The $\Delta m_s = 2$ signal is a septet at any temperature.¹⁸ This implicates the six-ring methylene hydrogens in any conformational change responsible for the spectral evolution.



The irreversible changes in the $\Delta m_s = 2$ region can be simulated by considering each spectrum to be a weighted sum of the limiting octet and nonet spectra (Figure 7). When done properly, this constitutes an example of the "distribution slicing" technique²⁰ that we have previously employed to analyze kinetics in frozen matrices. Figure 8 shows the results of fitting the data of Figure 7 to a collection of matrix sites that display a Gaussian distribution of Arrhenius activation energies. The width of the Gaussian (σ) is 0.6 kcal/mol, in excellent agreement with our previous analysis²⁰ of frozen solvent systems. If we assume $\log A = 13$ (Table II), the center of the Gaussian, and hence the most probable rate, corresponds to $E_a = 4.6$ kcal/mol.

Although we cannot unambiguously identify the process that corresponds to these activation parameters, a reasonable candidate is a conformational change involving the cyclohexene ring. Table

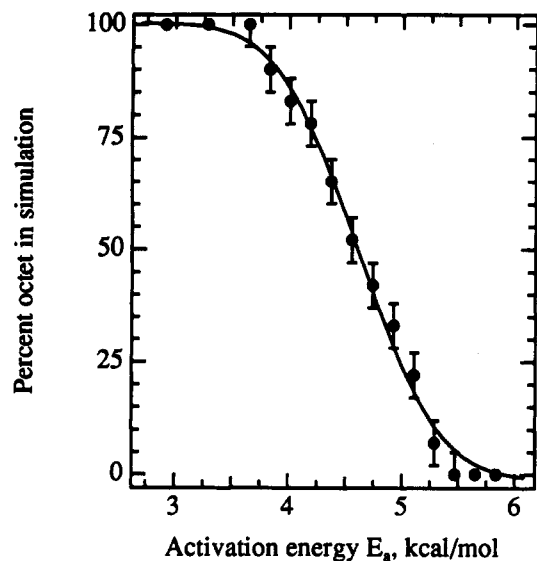
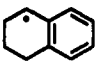




Figure 8. Plot of the simulation data from Figure 7 according to the distribution slicing method (ref 20). The curve is the best fit of the data to a Gaussian distribution of activation energies, centered at 4.6 kcal/mol with a width $\sigma = 0.6$ kcal/mol.

TABLE II: Arrhenius Parameters for Ring Inversion in Cyclohexenyl-Type Radicals

radical	E_a , kcal/mol	$\log A$
 20 ^a	7.2 ± 0.9	13.1 ± 0.7
 21 ^b	7.0 ± 0.9	13.1 ± 0.7
 22 ^b	2.4 ± 0.5	12.6 ± 0.8

^a Reference 21a. ^b Reference 21b.

II shows activation parameters for ring inversion processes in several cyclohexenyl-type radicals.²¹ The most closely related systems, **20** and **21**, show $E_a \sim 7$ kcal/mol, while the barrier for **22** is smaller. Certainly, the barrier we see is within a sensible range for a conformational process. One possible reason for it being lower than the best analogs is that **20** and **21** undergo a reversible process. Perhaps, in **19**, the system is initially formed in an unfavorable, high-energy state, and the barrier out of this conformation is lower than that for a typical, reversible process.

Surprisingly, the parent biradical **10** also shows temperature-dependent behavior (Figure 9). Photolysis of the diazene precursor at 77 K in MTHF gives a $\Delta m_s = 1$ spectrum with $|D/hc| = 0.0195$, $|E/hc| = 0.00175$ cm⁻¹. A nearly identical spectrum is observed in propylene glycol. Photolysis at 4.0 or 50.0 K gives a spectrum with $|D/hc| = 0.0192$, $|E/hc| = 0.00248$ cm⁻¹. On warming to 77.0 K, $|D/hc| = 0.0189$, $|E/hc| = 0.00148$ cm⁻¹. On warming to 86.0 K, $|D/hc| = 0.0176$, $|E/hc| = 0.00147$ cm⁻¹. These changes are all irreversible.

The $\Delta m_s = 2$ region of **10** shows reversible, temperature-dependent behavior (Figure 10). At 4.4 K a nonet, a_H 11.2 G, is observed.¹⁸ On warming past 30 K, a more complex $\Delta m_s = 2$ spectrum is observed. This spectrum is identical to that observed on photolysis at 77 K in MTHF or propylene glycol. On recooling below 20 K, the nonet is restored. Despite these changes, a Curie plot based on the total intensity of the $\Delta m_s = 2$ region is linear from 4 to 70 K.

The deuterated TMM **10-D₃** was prepared by photolysis of the diazene precursor. The $\Delta m_s = 2$ signal is a septet at any

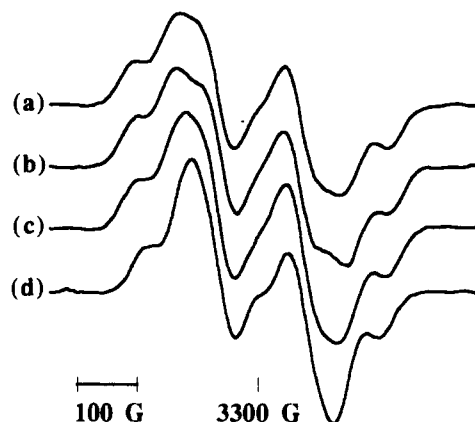
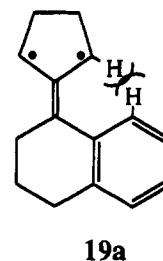


Figure 9. $\Delta m_s = 1$ spectra observed after photolysis of **10(N₂)** in MTHF: (a) photolysis at 77 K in liquid nitrogen, (b) photolysis at 50 K in the cryostat, (c) sample in (b) warmed to 77 K, (d) sample in (b) warmed to 86 K. The changes with temperature are irreversible.

temperature.¹⁸ This implies that the methyl hydrogens are solely responsible for the temperature-dependent behavior described above.²²

The irreversible decrease in D on warming is explained if the TMM is initially formed in a conformation with the phenyl ring substantially twisted from the plane of the TMM. Warming the sample apparently allows the phenyl and TMM to become more nearly coplanar.²⁵ The changes in the $\Delta m_s = 2$ region are reasonably explained by considering the effect of temperature on the methyl group. The nonet observed at low temperatures implies eight coupled hydrogens—six from the TMM and two from the CH₃. The $\Delta m_s = 2$ septet observed for **10-D₃** confirms this assignment. Apparently, at low temperatures the CH₃ is frozen in a conformation with one C–H bond in the plane of the TMM, as is typical for vinylic methyl groups.²³ On warming the sample, CH₃ rotation becomes rapid and a complex spectrum is observed.

One surprising feature of the series **17–19** is the trend in zfs D values (Table I), which runs completely contrary to our initial expectations based on presumed degree of planarity and thus biradical delocalization. Apparently, some other factor is influencing the D values, and we propose that this may be twisting of the TMM unit itself. Our calculations (see Experimental Section) do suggest substantial twisting of the TMMs (and the analogous fulvenes) due to steric interactions of the sort shown in **19a**, and the extent of twisting follows the series **19** > **18** > **17**. It is difficult to predict how such twisting will influence a TMM D value, but if our interpretation is correct, it apparently leads to a decrease in D . In light of this, it is dangerous to interpret the surprising result that $D(\mathbf{10}) \approx D(\mathbf{17})$.



Conclusions

Using the bis(TMM) strategy, the influence of twisting on the effectiveness of *m*-phenylene as a ferromagnetic coupling unit has been evaluated. Under conditions of modest twisting (**4**), *m*-phenylene is still an effective FC. Completely twisting both spin-containing units out of conjugation with the *m*-phenylene (**13**) leads to no interactions at all, and the SCs act independently.

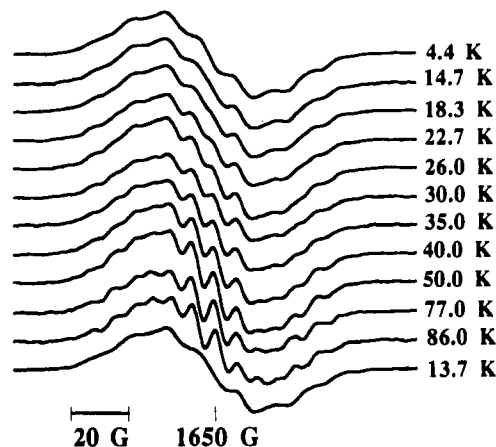


Figure 10. $\Delta m_s = 2$ spectra observed after photolysis of $10(N_2)$ at 4.2 K in MTHF. The changes with temperature are reversible.

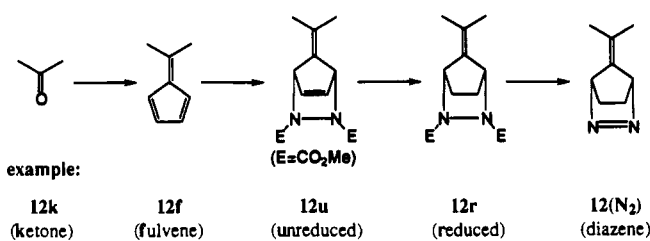
Interestingly, having one SC in plane and one SC completely out of plane as in **14** apparently still leads to ferromagnetic coupling. We propose a novel mechanism in which antiferromagnetic coupling between a center of negative spin density and a center of positive spin density leads to overall ferromagnetic coupling. The antiFC involved resembles the singlet biradical 90° twisted ethylene.

Several TMM biradicals have been studied as potential probes of conformational effects. The bulky substituent in **11** leads to a relatively large D value, consistent with the predicted loss of conjugation. The ring-constrained systems **17–19** display complex conformational behaviors, and their D values seem to reflect effects other than just degree of coplanarity between the TMM and the aromatic ring.

Experimental Section

General. Reactions were performed under an argon atmosphere. Tetrahydrofuran was distilled from sodium benzophenone ketyl. Methylene chloride was distilled from CaH_2 . Reported yields refer to material dried to constant weight under vacuum, typically 50 mTorr. Flash chromatography was on 230–400 mesh silica gel with the solvent indicated. All NMR shifts are reported as δ ppm downfield from TMS. 1H NMR was at 300 MHz in $CDCl_3$, and ^{13}C NMR was at 75 MHz in $CDCl_3$ using a GE QE-300 spectrometer. A range of peak positions indicates a multiplet of poorly resolved lines. IR spectra were recorded on a Perkin Elmer 1600 series instrument. MS refers to a 70-eV EI mass-selective detector (HP 5970) coupled to a HP 5890 GC unless otherwise indicated. Relative mass abundances (%) are given in parentheses (100 = base peak). FAB, DEI, 20-ev EI, and HRMS determinations were performed at the University of California, Riverside. UV spectra were taken using a Beckman DU-640 spectrometer. Elemental analysis was performed at Atlantic Microlabs, Norcross, GA. Melting points were obtained on a Thomas-Hoover apparatus and are uncorrected. EPR spectra were obtained on a Varian E-line Century Series spectrometer operating at X-band. EPR samples were prepared in either 2-methyltetrahydrofuran (MTHF, refluxed over CaH_2 , distilled, and vacuum transferred from sodium benzophenone ketyl) or propylene glycol (dried over Na_2SO_4 and distilled under vacuum) and degassed with several freeze–pump–thaw cycles. A liquid nitrogen-filled finger Dewar was used for experiments at 77 K. An Oxford Instruments ESR-900 liquid helium cryostat was used for variable-temperature experiments (3.8–135 K). Samples were photolyzed in the EPR cavity with the filtered, focused output (~ 307 – 386 nm) of a 500-W Hg arc lamp. Lamps, housings, lenses, and power supplies were obtained from Oriol Corp., Stratford, CT. Filters were obtained from Schott Optical Glass Co., Duryea, PA.

General Route to Diazenes. The diazene precursors for all the TMMs were synthesized via similar routes. The ketone starting material was converted to the fulvene, which was reacted with dimethyl azodicarboxylate (DMAD) and reduced to the biscarbamate. This was hydrolyzed and oxidized to the diazene (see sequence below). All diazenes are stored at $-20^\circ C$ in CH_2Cl_2 solution.



(for difunctional compounds, f refers to the bisfulvene, etc.)

General Preparation of Fulvenes. Most of the fulvenes were synthesized by condensation of the corresponding ketone with CpMgBr in refluxing THF. CpMgBr was prepared from MeMgBr and cyclopentadiene and was assumed to have an effective MW of about 400.²⁶ A representative fulvene preparation using CpMgBr is given below.

General Preparation of Reduced DMAD Adducts. Most fulvenes were reacted with a slight excess of DMAD in CH_2Cl_2 at room temperature and then reduced with diimide generated from potassium azodicarboxylate (PADC). Occasionally the intermediate unreduced DMAD adduct was isolated. A general preparation is given below.

General Preparation of Diazenes. Most of the reduced DMAD adducts were refluxed with KOH in isopropyl alcohol and then oxidized with nickel peroxide (NiO_x) in CH_2Cl_2 at $0^\circ C$. A representative preparation is given below. An alternate oxidation with $CuCl_2$ is also given.

1,3-Dipivaloylbenzene (13k). A 1.28-g portion of 1,3-dicyanobenzene (10.0 mmol) was dissolved in 40 mL of dry THF in a flame-dried flask under argon and then 11.5 mL of 2.0 M *t*-BuMgCl/ether (23.0 mmol, 2.3 equiv) was added, followed immediately by 36 mg (0.40 mmol, 0.04 equiv) of $CuCN$.²⁷ The mixture was rapidly heated to reflux. After 21 h, the solution was cooled to room temperature and carefully quenched with 5 mL of water followed by 30 mL of 15% sulfuric acid. The biphasic mixture was stirred at room temperature for 22 h and then 25 mL of ether was added and the layers shaken and separated. The aqueous layer was extracted with 25 mL of ether. The organic extracts were combined, dried ($MgSO_4$), filtered, and chromatographed (5% ethyl acetate/hexanes) to provide 0.94 g (38%) of a white solid. An analytical sample was recrystallized from ethanol/water, long white needles, mp 48.5 – $49.0^\circ C$. 1H NMR δ 8.04 (dt, $J = 1.8, <1$ Hz, 1H), 7.80 (dd, $J = 7.8, 1.8$ Hz, 2H), 7.46 (dt, $J = 7.8, <1$ Hz, 1H), 1.37 (s, 18H). ^{13}C NMR δ 208.27, 138.19, 130.04, 127.87, 127.3, 44.19, 27.88. IR (NaCl plate, film) 1677 cm^{-1} . MS M^{+} 246 (1), 190 (23), 189 (100), 57 (48). HRMS calcd for $C_{16}H_{22}O_2$: 246.1620, found 246.1618. Anal. Calcd for $C_{16}H_{22}O_2$: C 78.01, H 9.00, found C 77.96, H 9.10.

Ketal from 3-Acetylbenzotrile. A 2.50-g portion of 3-acetylbenzotrile (17.22 mmol) was dissolved in 50 mL of benzene. Ethylene glycol (9.6 mL, 10 equiv) and 330 mg of p-TsOH· H_2O (1.73 mmol, 0.1 equiv) were added. The mixture was heated to reflux using a Dean-Stark trap to remove water. After 5 h of reflux the cooled solution was quenched with 25 mL each of water and saturated aqueous (satd. aq.) NaCl. The layers were shaken and separated, and the aqueous layer was extracted with 2×25 mL of benzene. The organic extracts were combined and rotoevaporated, giving a quantitative yield of a colorless solid. 1H NMR δ 7.81 (t, $J = 1.7$ Hz, 1H), 7.75 (dt, $J = 7.8, 1.5$ Hz, 1H), 7.60 (dt, $J = 7.5, 1.4$ Hz, 1H), 7.48 (t, $J = 7.7$ Hz, 1H), 4.08

(m, 2H), 3.78 (m, 2H), 1.64 (m, 3H). ^{13}C NMR δ 144.98, 131.33, 129.69, 128.97, 128.90, 118.57, 112.09, 107.73, 64.47, 27.28. MS $[\text{M}-\text{CH}_3]^+$ 174 (100), 130 (87), 102 (46).

3-Acetyl-pivalophenone (14k). A 3.34-g portion of cyano ketal (17.7 mmol) was dissolved in 50 mL of dry THF in a flame-dried flask under argon and 13.2 mL of 2.0 M *t*-BuMgCl/ether (26.4 mmol, 1.5 equiv) was added, followed immediately by 41 mg (0.46 mmol, 0.026 equiv) of CuCN.²⁷ The mixture was rapidly heated to reflux. After 2.5 h, the solution was cooled to room temperature and carefully quenched with 20 mL of water and then 50 mL of 15% sulfuric acid. The biphasic mixture was stirred for 13 h at room temperature. The layers were shaken and separated, and the aqueous layer was extracted with 2 \times 50 mL of ether. The organic layers were combined, dried (MgSO_4), and filtered through silica (5:1 hexanes:ethyl acetate), providing 3.25 g (85%) of a clear colorless oil. ^1H NMR δ 8.28 (dt, $J = <0.5, 1.8$ Hz, 1H), 8.06 (ddd, $J = 7.5, 1.8, 1.2$ Hz, 1H), 7.89 (ddd, $J = 7.5, 1.8, 1.2$ Hz, 1H), 7.53 (dt, $J = <0.5, 7.5$ Hz, 1H), 2.64 (s, 3H), 1.37 (s, 9H). ^{13}C NMR δ 208.12, 197.04, 138.69, 136.69, 131.87, 130.20, 128.27, 127.39, 44.03, 27.70, 26.43. IR (NaCl plate, film) 1685 cm^{-1} . MS M^{++} 204 (1), 148 (33), 147 (100), 57 (38). HRMS calcd for $\text{C}_{13}\text{H}_{16}\text{O}_2$: 204.1150, found 204.1162. Anal. Calcd for $\text{C}_{13}\text{H}_{16}\text{O}_2$: C 76.44, H 7.90, found C 76.18, H 7.92.

Representative Preparation of Fulvenes from Ketones and CpMgBr: 6-(*p*-Methoxyphenyl)-6-methylfulvene (8).²⁸ A 1.00-g (6.67 mmol) portion of *p*-methoxyacetophenone and 8.0 g of CpMgBr (3 equiv) were refluxed in 50 mL of dry THF under argon. After 3.5 h, the solution was quenched into 50 mL of satd. aq. NH_4Cl and 10 mL of water. The layers were shaken and separated, and the aqueous layer was extracted with 25 mL of ether. The organic layers were combined, dried (MgSO_4), and filtered. The residue was chromatographed (1% ether/hexanes) to provide 1.109 g (84%) of an orange solid, mp 65.5–66.5 $^\circ\text{C}$ (lit. mp²⁸ 64.0–65.5 $^\circ\text{C}$). MS M^{++} 198 (100), 183 (97). HRMS calcd for $\text{C}_{14}\text{H}_{14}\text{O}$: 198.1045, found 198.1050. UV λ_{max} (CH_2Cl_2) 326 nm. X-ray crystals were grown by slow evaporation from a hot pentane solution.

6-(*p*-Bromophenyl)-6-*tert*-butylfulvene (9). From 1.02 g of *p*-bromopivalophenone²⁹ and 5.1 g of CpMgBr, 2-h reflux, was isolated 981 mg (80%) of a pale-orange solid, mp 105.0–106.0 $^\circ\text{C}$. ^1H NMR δ 7.44 (d, $J = 8.7$ Hz, 2H), 6.99 (d, $J = 8.7$ Hz, 2H), 6.85 (ddd, $J = 5.4, 2.1, 1.2$ Hz, 1H), 6.55 (ddd, $J = 5.4, 2.1, 1.8$ Hz, 1H), 6.22 (ddd, $J = 5.4, 2.1, 1.2$ Hz, 1H), 5.52 (ddd, $J = 5.4, 2.1, 1.8$ Hz, 1H), 1.31 (s, 9H). ^{13}C NMR δ 162.15, 143.35, 141.16, 133.10, 129.96, 128.71, 126.26, 122.16, 120.73, 38.04, 33.12. MS M^{++} 288, 290 (100:100), 273, 275 (33:33), 194 (30). HRMS calcd for $\text{C}_{16}\text{H}_{17}\text{Br}$: 288.0514, found 288.0507. UV λ_{max} (CH_2Cl_2 or pentane) 252, 338 (sh) nm. X-ray crystals were grown by allowing a hot pentane solution to cool at room temperature.

6-Phenyl-6-methylfulvene (10f). From 0.49 mL of acetophenone and 5.0 g of CpMgBr, 3-h reflux, was isolated 683 mg (97%) of an orange oil. ^1H NMR δ 7.52 (m, 5H), 6.80 (d, $J = 5.1$ Hz, 1H), 6.73 (d, $J = 5.1$ Hz, 1H), 6.64 (d, $J = 5.1$ Hz, 1H), 6.36 (d, $J = 5.1$ Hz, 1H), 2.68 (s, 3H). ^{13}C NMR δ 149.65, 143.30, 141.90, 131.75, 131.41, 129.12, 128.10, 127.78, 123.61, 120.98, 22.53. MS M^{++} 168 (54), 153 (100). HRMS calcd for $\text{C}_{13}\text{H}_{12}$: 168.0939, found 168.0934. UV λ_{max} (CH_2Cl_2) 300, ~378 (sh) nm.

Fulvene 10f-D₃. Prepared as for 10f from acetophenone-D₃ (Aldrich, 98 atom % D). ^1H NMR identical to that of 10f, except no singlet at 2.68 ppm. ^{13}C NMR identical to that of 10f, except singlet at 22.53 ppm replaced by a septet, $J_{\text{C-D}} = 19.4$ Hz. MS M^{++} 171 (65), 153 (100). HRMS calcd for $\text{C}_{13}\text{H}_9\text{D}_3$: 171.1127, found 171.1133.

6-Phenyl-6-*tert*-butylfulvene (11f). From 1.00 g of pivalophenone and 7.4 g of CpMgBr, 1.5-h reflux, was isolated 686 mg

(53%) of a pale-orange solid, mp 34.0–35.0 $^\circ\text{C}$. ^1H NMR δ 7.28 (m, 3H), 7.10 (m, 2H), 6.87 (dm, $J = 5.4$ Hz, 1H), 6.54 (dt, $J = 5.4, 1.8$ Hz, 1H), 6.19 (dm, $J = 5.4$ Hz, 1H), 5.54 (dt, $J = 5.4, 1.8$ Hz, 1H), 1.33 (s, 9H). ^{13}C NMR δ 163.89, 143.06, 142.31, 132.73, 128.20, 128.17, 126.73, 126.57, 126.55, 122.15, 38.14, 33.17. MS M^{++} 210 (40), 195 (100), 180 (52), 165 (67). HRMS calcd for $\text{C}_{16}\text{H}_{18}$: 210.1409, found 210.1406. UV λ_{max} (CH_2Cl_2) 267, 370 nm.

Bisfulvene 13f. From 1.00 g of diketone 13k and 9.7 g of CpMgBr, 4-h reflux, was isolated 956 mg (69%) of a pale-orange solid. ^1H NMR δ 7.24 (t, $J = 7.5$ Hz, 1H), 7.04 (m, 2H), 6.86 (m, 3H), 6.53 (m, 2H), 6.21 (m, 2H), 5.59 (m, 2H), 1.34 (s, 9H), 1.33 (s, 9H). ^{13}C NMR δ 163.6–122.0 (m), 38.19, 38.12, 33.24, 33.20. The 1.34 and 1.33 ppm peaks in the ^1H spectrum ($\Delta\delta$ 2.5 Hz at 25 $^\circ\text{C}$) reversibly coalesce at 70 $^\circ\text{C}$ in toluene- d_6 . MS M^{++} 342 (81), 285 (70), 229 (100). HRMS calcd for $\text{C}_{26}\text{H}_{30}$: 342.2348, found 342.2362.

Bisfulvene 14f. From 0.673 g of diketone 14k and 8.0 g of CpMgBr, 5-h reflux, was isolated 590 mg (60%) of the bisfulvene as an orange oil. ^1H NMR δ 7.33 (d, $J = 5.1$ Hz, 2H), 7.13 (m, 1H), 7.11 (m, 1H), 6.87 (ddd, $J = 5.6, 2.1, 1.2$ Hz, 1H), 6.63 (m, 1H), 6.56 (m, 2H), 6.48 (m, 1H), 6.23 (dt, $J = 4.0, 1.5$ Hz, 1H), 6.20 (ddd, $J = 7.1, 3.8, 1.6$ Hz, 1H), 5.75 (dt, $J = 5.4, 1.8$ Hz, 1H), 2.55 (s, 3H), 1.35 (s, 9H). ^{13}C NMR δ 163.12, 149.48, 143.52, 143.33, 142.03, 140.62, 132.93, 131.90, 131.65, 129.03, 128.52, 128.12, 127.40, 126.43, 126.40, 123.48, 122.22, 121.07, 38.23, 33.22, 22.71. MS M^{++} 300 (32), 285 (74), 243 (100). HRMS calcd for $\text{C}_{23}\text{H}_{24}$: 300.1878, found 300.1883.

Fulvene from Benzocyclobutenone (17f). Attempted preparation from the ketone and CpMgBr did not give the desired product. NMR evidence suggests that the four-membered ring opens. A 0.480-g portion of benzocyclobutenone^{30,31} (4.06 mmol) was dissolved in 4 mL of methanol under argon. A 0.84-mL portion of cyclopentadiene (10.19 mmol, 2.5 equiv) and 1.85 mL of pyrrolidine (20.44 mmol, 5.0 equiv) were added, and the mixture was stirred.³² After 1 h at room temperature, the orange-brown solution was quenched with 1.25 mL of acetic acid (21.84 mmol, 5.4 equiv) and diluted with 20 mL each of ether and water. The layers were separated, and the aqueous layer was extracted with 2 \times 20 mL of ether. The organic extracts were combined, washed with 20 mL of satd. aq. NaCl, dried (MgSO_4), and filtered. The residue was chromatographed (1% ether/hexanes) yielding 313 mg (46%) of a dark-orange solid, mp 74.0–75.0 $^\circ\text{C}$. ^1H NMR δ 7.27 (m, 4H), 6.66 (dt, $J = 5.1, 1.8$ Hz, 1H), 6.54 (m, 2H), 6.37 (dt, $J = 5.1, 1.8$ Hz, 1H), 3.87 (s, 2H). ^{13}C NMR δ 146.76, 146.71, 143.74, 136.05, 131.70, 131.54, 131.19, 128.11, 123.06, 121.37, 121.32, 121.01, 38.12. MS M^{++} 166 (49), 165 (100). HRMS calcd for C_{13}H_9 : 165.0704, found 165.0699. UV λ_{max} (CH_2Cl_2) 280 (sh), 293, 307, 329, 341 nm.

Fulvene from 1-Indanone, 18f. From 1.00 g of indanone and 9.1 g of CpMgBr, 4.5-h reflux, was isolated 853 mg (62%) of a dark orange-red solid, mp 70.5–72.0 $^\circ\text{C}$. ^1H NMR δ 7.95 (d, $J = 7.2$ Hz, 1H), 7.28 (m, 3H), 6.92 (m, 1H), 6.52 (m, 2H), 6.47 (m, 1H), 3.25 (dd, $J = 6.6, 5.7$ Hz, 2H), 3.03 (dd, $J = 6.6, 5.7$ Hz, 2H). ^{13}C NMR δ 155.22, 151.40, 140.13, 137.47, 131.59, 130.41, 129.90, 127.06, 126.45, 125.56, 123.09, 119.47, 32.56, 30.24. MS M^{++} 180 (93), 165 (100). HRMS calcd for $\text{C}_{14}\text{H}_{12}$: 180.0939, found 180.0947. UV λ_{max} (CH_2Cl_2) 345 nm.

Fulvene from α -Tetralone, 19f. From 1.00 mL of α -tetralone and 9.0 g of CpMgBr, 4.5-h reflux, was isolated 973 mg (67%) of a dark orange-red oil. ^1H NMR δ 7.54 (dm, $J = 7.5$ Hz, 1H), 7.28–7.09 (m, 3H), 6.65–6.52 (m, 4H), 2.99 (t, $J = 6.6$ Hz, 2H), 2.78 (t, $J = 6.6$ Hz, 2H), 1.92 (quintet, $J = 6.6$ Hz, 2H). ^{13}C NMR δ 149.67, 140.92, 140.80, 135.89, 132.09, 131.59, 130.97, 129.05, 128.21, 125.48, 123.61, 120.93, 30.69, 29.44, 23.18. MS M^{++} 194 (100), 165 (88). HRMS calcd for $\text{C}_{15}\text{H}_{14}$: 194.1096, found 194.1094. UV λ_{max} (CH_2Cl_2) 324 nm.

Fulvene 19f-D₂. Prepared as for **19f** from α -tetralone-D₂.³³ ¹H NMR identical to that of **19f**, except methylene peaks replaced by peaks at 2.83 and 1.96 ppm (each t, $J = 6.3$ Hz, 2H). ¹³C NMR identical to that of **19f**, except methylene peaks replaced by singlets at 29.46, 23.08 ppm and quintet at 30.12 ppm, $J_{C-D} = 19.7$ Hz. MS M^{++} 196 (100), 180 (56), 167 (55). HRMS calcd for C₁₅H₁₂D₂: 196.1221, found 196.1215.

DMAD Addition and Diimide Reduction: General Procedure.

10r. A 0.685-g portion of fulvene **10f** (4.07 mmol) and 0.595 g of DMAD (4.07 mmol, 1.0 equiv) were stirred in 25 mL of dry CH₂Cl₂ under argon. (For some compounds, as noted, the unreduced DMAD adduct was isolated by chromatography at this point. We have found, however, that immediate reduction of the adduct without isolation is generally more efficient.) After 1 h, the solution was cooled in an ice-water bath, and 1.98 g of PADC (10.19 mmol, 2.5 equiv) was added. A solution of 1.2 mL of acetic acid (21.0 mmol, 5.2 equiv) in 5 mL of CH₂Cl₂ was added dropwise over 20 min. The mixture was stirred as the flask was allowed to warm to room temperature. Typically the reaction with PADC was allowed to stir overnight before workup. The mixture was quenched with 20 mL of water. The layers were shaken and separated, and the aqueous layer was extracted with 25 mL of CH₂Cl₂. The organic layers were combined, dried (K₂CO₃), filtered, and rotoevaporated. The residue was chromatographed (2:1 hexanes:ethyl acetate) to provide 1.018 g (79%) of a sticky yellow solid. ¹H NMR δ 7.30 (m, 3H), 7.18 (dm, $J = 6.6$ Hz, 2H), 5.17–4.42 (br m, 2H), 3.78 and 3.70 (each br s, tot 6H), 2.10 (s, 3H), 2.2–1.6 (br m, 4H). ¹³C NMR δ 158.6, 157.90, 140.55, 134.86, 127.83, 127.00, 124.90, 59.0 (br m), 52.72 (m), 28.1 (br m), 26.5 (br m), 19.9 (br). MS M^{++} 316 (19), 229 (61), 169 (87), 168 (100). HRMS calcd for C₁₇H₂₀N₂O₄: 316.1423, found 316.1413.

10r-D₃. Prepared as for **10r**. ¹H NMR identical to that of **10r**, except no singlet at 2.10 ppm. ¹³C NMR identical to **10r**, except no broad peak at 20.24 ppm. Septet for CD₃ carbon too weak to observe. MS M^{++} 319 (19), 232 (41), 171 (100), 170 (83), 59 (64). HRMS calcd for C₁₇H₁₇D₃N₂O₄: 319.1611, found 319.1625.

11u. From 0.588 g of fulvene **11f** (2.80 mmol) was isolated by chromatography (5:1 to 3:1 hexanes:ethyl acetate) 881 mg (81%) of a white solid. ¹H NMR δ 7.29 (m, 3H), 7.1–6.5 (br m, 4H), 6.0–5.6 (br m, 1H), 4.7–4.2 (br m, 1H), 3.81 (br s, 3H), 3.67 (br s, 3H), 1.11 (s, 9H). ¹³C NMR δ 159.10, 140.84, 140.29, 129.87, 128.78, 128.31, 127.58, 126.58, 66.5 (br), 63.4 (br), 53.44, 35.39, 30.74.

11r. From 0.881 g of **11u** (2.47 mmol) was isolated 872 mg (98%) of a white foamy solid. ¹H NMR δ 7.29 (m, 3H), 7.1–6.8 (br m, 2H), 5.5–5.1 (br m, 2H), 3.81 (br s, 3H), 3.68 (br s, 3H), 2.2–1.4 (br m, 4H), 1.14 (s, 9H). ¹³C NMR δ 157.4 (br), 140.88, 134.86, 128.62, 128.06, 127.44, 126.59, 62.2 (br), 59.0 (br), 53.30, 52.97, 36.15, 31.20, 26.8 (v br). MS M^{++} 358 (22), 301 (100), 257 (90). HRMS calcd for C₂₀H₂₆N₂O₄: 358.1893, found 358.1895.

13u. From 0.845 g of bisfulvene **13f** (2.47 mmol) was isolated by chromatography (2:1 to 1:1 hexanes:ethyl acetate) 1.553 g (99%) of a white foamy solid. ¹H NMR δ 7.3–7.2 (m, 1H), 7.0–6.5 (br m, 7H), 6.0–4.2 (v br m, 4H), 3.9–3.6 (m, 12H), 1.2–1.0 (m, 18 H). ¹³C NMR δ 159.07 (br), 140.1–126.8 (m), 65.89 (br), 63.5 (br), 53.32, 53.18, 53.14, 35.47, 35.32, 30.96, 30.78, 30.69, 30.64, 30.53.

13r. From 1.553 g of **13u** (2.45 mmol) was isolated 1.514 g (97%) of a white foamy solid. ¹H NMR δ 7.27 (t, $J = 7.8$ Hz, 1H), 6.90 (m, 2H), 6.55 (m, 1H), 5.41–5.15 (br m, 4H), 3.75 (m, 12H), 1.97 (br m, 4H), 1.72 (br m, 4H), 1.15 (m, 18H). ¹³C NMR δ 158.3, 157.0, 140.38, 140.05, 139.93, 139.87, 138.97, 134.76, 134.72, 134.60, 126.62 (br m), 62.1 (br m), 61.5 (br m), 58.9 (br m), 53.3 (br m), 36.05, 35.94, 31.05, 30.82, 26.72 (br

m). DEI-MS M^{++} 638 (8), 538 (38), 537 (100), 375 (32). HRMS calcd for C₃₄H₄₆N₄O₈: 638.3316, found 638.3316.

14u. From 0.590 g of bisfulvene **14f** (1.96 mmol) was isolated by chromatography (2:1 to 1:2 hexanes:ethyl acetate) 455 mg (39%) of a yellow oil which did not solidify. ¹H NMR δ 7.4–4.2 (m, 12H), 3.9–3.6 (m, 12H), 2.0 (m, 3H), 1.12 (s, 9H). ¹³C NMR δ 158.9 (br), 143.7–125.5 (m), 65.9 (br), 63.5 (br), 54.8–52.4 (m), 30.57.

14r. From 0.455 g of **14u** (0.768 mmol) was isolated 403 mg (88%) of a pale-yellow foamy solid. ¹H NMR δ 7.28 (m, 1H), 7.13 (m, 1H), 6.88 (m, 1H), 6.81 (m, 1H), 5.49–4.43 (br m, 4H), 3.80 (m, 12H), 2.12 (2s, $\Delta\delta = 2.6$ Hz, tot 3H), 2.2–1.4 (br m, 8H), 1.15 (2s, $\Delta\delta = 3.9$ Hz, tot 9H). ¹³C NMR δ 158.5, 157.2, 140.7 (br), 139.02, 135.44, 135.28, 134.92, 127.76, 127.67, 127.47, 127.32, 127.1 (br), 126.99, 125.63, 124.72, 61.9 (br), 49.1 (br), 53.0 (br m), 36.02, 31.01, 26.6 (br m), 20.1 (br). DEI-MS M^{++} 596 (20), 496(31), 495 (100), 333 (40). HRMS calcd for C₃₁H₄₀N₄O₈: 596.2846, found 596.2855.

17r. From 0.306 g of fulvene **17f** (1.84 mmol) was isolated by chromatography (3:2 hexanes:ethyl acetate) 416 mg (72%) of a yellow foamy solid. ¹H NMR δ 7.23 (m, 4H), 5.38–4.42 (br m, 2H), 4.03–3.35 (m, 8H), 2.36–1.49 (br m, 4H). ¹³C NMR δ 144.6–119.2 (m), 59.59 (br), 53.25 (m), 36.75, 28.33 (v br), 26.78 (br). MS M^{++} 314 (50), 167 (94), 166 (100), 165 (87), 59 (100). HRMS calcd for C₁₇H₁₈N₂O₄: 314.1267, found 314.1275.

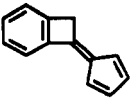
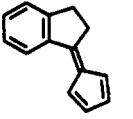
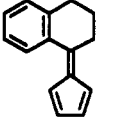
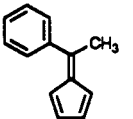
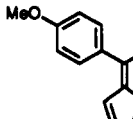
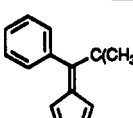
18r. From 0.578 g of fulvene **18f** (3.21 mmol) was isolated by chromatography (2:1 to 1:2 hexanes:ethyl acetate) 442 mg (42%) of an off-white foamy solid. ¹H NMR δ 7.80–7.06 (m, 4H), 5.74–4.57 (m, 2H), 4.00–3.37 (m, 6H), 3.15–2.56 (m, 4H), 2.36–1.45 (m, 4H). ¹³C NMR δ 147.9–122.8 (m), 60.87 (br), 57.74 (br), 53.38 (br), 30.00, 29.90, 27.17 (v br). 20 eV EI-MS M^{++} 328 (4), 180 (100). HRMS calcd for C₁₈H₂₀N₂O₄: 328.1423, found 328.1408.

19r. From 0.685 g of fulvene **19f** (3.53 mmol) was isolated by chromatography (2:1 hexanes:ethyl acetate) 800 mg (66%) of a sticky pale-orange solid. ¹H NMR δ 7.18 (m, 4H), 5.70–4.55 (m, 2H), 3.77 (m, 6H), 3.05–2.30 (m, 4H), 2.30–1.44 (m, 6H). ¹³C NMR δ 138.8–125.6 (m), 59.36 (br), 53.14 (br), 29.25, 29.11, 26.90 (v br), 23.77. 20 eV EI-MS M^{++} 342 (4), 194 (100). HRMS calcd for C₁₉H₂₂N₂O₄: 342.1580, found 342.1563.

19r-D₃. Prepared as for **19r**. ¹H NMR identical to that of **19r**, except peak at 3.05–2.30 ppm (m, 4H) replaced with a peak at 2.76 (m, 2H). ¹³C NMR identical to that of **19r**, except methylene peaks replaced by singlets at 29.03 and 23.42 ppm. Quintet for CD₃ carbon too weak to observe. FAB-MS M^{++} 344. HRMS calcd for C₁₉H₂₀D₃N₂O₄: 344.1705, found 344.1693.

Representative Diazene Preparation Using NiO_x Oxidant: Diazene 10(N₂). A 0.218-g portion of **10r** (0.689 mmol) and 673 mg of powdered 87% KOH (15 equiv) were degassed 3 times on the vacuum line and purged for 10 min with argon. Then 20 mL of degassed isopropyl alcohol (30 min of argon bubbling) was added via cannula, and the mixture was stirred and heated to reflux for 90 min. The mixture was cooled to room temperature, and 0.87 g of NaHCO₃ (15 equiv) was added. The mixture was stirred for 1 h at room temperature, and the solvent was pumped off overnight. The brown residue was partitioned between 25 mL each of water and CH₂Cl₂ with gentle shaking, and the layers were separated. The aqueous layer was extracted with 25 mL of CH₂Cl₂. The organic layers were combined, dried (K₂CO₃), filtered, and cooled in an ice-water bath. A 1.17-g portion of NiO_x was added, and the mixture was stirred at 0 °C in the dark for 1 h. The mixture was filtered through Celite and rotoevaporated to provide 80 mg (58%) of a pale-yellow film. ¹H NMR δ 7.32 (m, 3H), 7.12 (m, 2H), 5.50 (d, $\Delta\delta = 2.7$ Hz, 1H), 5.27 (d, $\Delta\delta = 2.7$ Hz, 1H), 2.00 (s, 3H), 1.75 (m, 2H), 1.16 (m, 2H). ¹³C NMR δ 141.48, 140.59, 128.11, 127.31, 127.24, 124.89, 74.52, 74.40, 21.28, 21.17, 19.77. UV λ_{max} (CH₂Cl₂) 297, 342 (sh) nm.

TABLE III: MM2-Calculated Lowest Energy Structures of Phenyl-Substituted Fulvenes^c

fulvene	φ_1^a	φ_1'	φ_2	φ_2'	φ_3	φ_3'	$d_1, \text{\AA}$	$d_2, \text{\AA}$
	0.0	0.0	0.0	0.0	0.0	0.0	2.604	1.472
	19.6	17.1	3.0	3.0	2.3	3.6	2.131	1.468
	41.3	39.2	4.5	4.5	2.6	6.4	2.322	1.476
	71.1	70.5	1.7	0.9	1.1	0.3	2.993	1.473
	70.2	69.6	1.7	1.0	1.1	0.4	2.987	1.472
	90.0	89.8	0.0	0.0	0.0	0.0	3.435 ^b 3.422	1.474

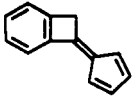
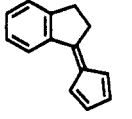
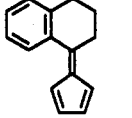
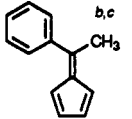
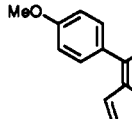
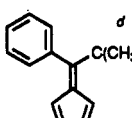
^a All values of φ (degrees) are reported as deviations from 0° or 180°, whichever was closer. ^b Two approximately equal H-H distances were found. ^c MM2 as implemented in MacroModel version 3.5a was used.

Diazene 10(N₂)-D₃. This compound was prepared as for 10(N₂). ¹H NMR was identical to that of 10(N₂), except no singlet at 2.00 ppm. ¹³C NMR was identical to that of 10(N₂), except no singlet at 19.77 ppm. The septet for the CD₃ carbon was observed but poorly resolved from baseline noise.

Representative Diazene Preparation Using CuCl₂ Oxidant: Diazene 11(N₂). A 0.292-g portion of 11r (0.815 mmol) and 787 mg of powdered 87% KOH (15 equiv) were degassed 3 times on the vacuum line and purged for 10 min with argon. Then 25 mL of degassed isopropyl alcohol (30 min of argon bubbling) was added via cannula and the mixture stirred and heated to reflux for 90 min. The mixture was cooled to room temperature and quenched with 20 mL of cold water. The solution was acidified to pH ≤ 2 with 1.0 mL of concentrated HCl and adjusted to pH ~ 6.0 with 3 N NH₄OH. The pale-yellow solution was treated dropwise with 2.2 mL of satd. aq. CuCl₂, giving a dark-brown solution. After 30 min, the pH was adjusted to ~5 with 3 N NH₄OH, producing a light-brown precipitate. This was suction filtered (30-mL medium fritted funnel) and rinsed with 50 mL of 3 N NH₄OH, giving a blue filtrate. The retained yellow solid was rinsed with 25 mL of CH₂Cl₂, giving a pale-yellow solution of the diazene. This was chromatographed (1:1 hexanes:ethyl acetate), although this step appears not to increase the purity of the diazene significantly and may be skipped. ¹H NMR δ 7.26 (m, 3H), 6.90 (m, 2H), 5.82 (d, $\Delta\delta$ = 3.0 Hz, 1H), 4.52 (d, $\Delta\delta$ = 3.0 Hz, 1H), 1.81 (m, 1H), 1.55 (m, 1H), 1.09 (s, 9H), 0.93 (m, 2H). ¹³C NMR δ 141.39, 140.37, 139.02, 128.26, 127.63, 127.24, 126.40, 77.41, 73.65, 36.09, 30.99, 21.14, 20.57. UV λ_{\max} (CH₂Cl₂) 340 nm.

Bisdiazene 13(N₂)₂. From 0.241 g of 13r (0.377 mmol), 734 mg of KOH, and 1.3 g of NiO_x was isolated 124 mg (82%) of a yellow solid. ¹H NMR δ 7.24 (m, 1H), 6.86 (m, 2H), 6.45 (m, 1H), 5.83 (s, 2H), 4.60–4.48 (m, 2H), 1.88–1.40 (br m, 4H), 1.2–0.8 (br m, 4H), 1.12–1.08 (m, 18H). ¹³C NMR δ 128.8–

TABLE IV: AM1-Calculated Lowest Energy Structures of Phenyl-Substituted Fulvenes^f

fulvene	φ_1^a	φ_1'	φ_2	φ_2'	φ_3	φ_3'	$d_1, \text{\AA}$	$d_2, \text{\AA}$
	0.0	0.0	0.0	0.0	0.0	0.0	2.627	1.472
	0.1	0.0	0.1	0.1	0.0	0.0	1.908	1.461
	35.9	34.9	5.5	5.8	3.9	7.4	2.132	1.461
	49.6	48.5	2.3	2.1	1.2	3.2	2.350	1.466
	48.0	46.8	2.8	2.5	1.7	3.7	2.323	1.463
	89.6	89.9	0.0	0.1	0.0	0.0	3.440 ^e 3.450	1.475

^a All values of φ (degrees) are reported as deviations from 0° or 180°, whichever was closer. ^b The minimization began from a structure with $\varphi_1, \varphi_2 \sim 57^\circ$. ^c Convergence criterion was set to 0.001 kcal/mol. ^d The minimization began from a structure with $\varphi_1, \varphi_2 \sim 73^\circ$. ^e Two approximately equal H-H distances were found. ^f The MM2-minimized structures were used to start the minimization, except where indicated. MOPAC as implemented in InsightII version 2.1.2 (BioSymb) was used with the following parameters: BFGS minimization type, line minimizer off, PRECISE keyword activated, 0.01 kcal/mol convergence criterion. Frequency calculations showed that all structures are true minima; all elements of the diagonalized force constant matrix were positive.

126.6 (m), 77.4 (m), 73.65, 31.16, 31.02, 29.46, 28.88, 21.18, 21.12, 20.64, 20.43. UV λ_{\max} (CH₂Cl₂) 342 (sh) nm.

Bisdiazene 14(N₂)₂. From 0.194 g of 14r (0.326 mmol), 635 mg of KOH, and 1.11 g of NiO_x was isolated 93 mg (79%) of a yellow solid. ¹H NMR δ 7.27 (m, 1H), 7.04 (m, 1H), 6.84 (m, 1H), 6.62 (m, 1H), 5.84 (m, 1H), 5.51 (m, 1H), 5.22 (m, 1H), 4.55 (m, 1H), 2.01 and 1.99 (each s, total 3H), 1.92–1.47 (br m, 4H), 1.34–0.81 (br m, 4H), 1.13 and 1.11 (each s, total 9H). ¹³C NMR δ 141.8 (m), 140.58–140.37 (m), 139.95, 127.76–127.28 (m), 125.83–125.53 (m), 77.61, 77.51, 77.44, 74.62, 74.60, 74.48, 74.43, 73.81, 36.25, 31.09, 31.36–21.11 (m), 20.75 (br m), 20.02–19.82 (m). UV λ_{\max} (CH₂Cl₂) 342 (sh) nm.

Diazene 17(N₂). From 0.237 g of 17r (0.754 mmol), 733 mg of KOH, and 1.28 g of NiO_x was isolated 114 mg (77%) of a yellow solid. ¹H NMR δ 7.20 (m, 4H), 5.60 (d, $\Delta\delta$ = 2.4 Hz, 1H), 5.34 (d, $\Delta\delta$ = 2.7 Hz, 1H), 3.52 (s, 2H), 1.75 (m, 2H), 1.22 (m, 2H). ¹³C NMR δ 144.78, 142.87, 135.17, 134.16, 128.84, 127.53, 122.75, 119.07, 74.61, 74.49, 36.78, 21.50, 21.29. UV λ_{\max} (CH₂Cl₂) 246, 256, 289, 297, 327, 340 nm.

Diazene 18(N₂). From 0.200 g of 18r (0.609 mmol), 590 mg of KOH, and 1.04 g of NiO_x was isolated 51 mg (40%) of a yellow solid. ¹H NMR δ 7.49 (m, 1H), 7.22 (m, 3H), 5.97 (d, $\Delta\delta$ = 2.7 Hz, 1H), 5.42 (d, $\Delta\delta$ = 2.7 Hz, 1H), 2.94 (m, 2H), 2.70 (m, 2H), 1.76 (m, 2H), 1.21 (m, 2H). ¹³C NMR δ 147.58, 139.18, 135.55, 129.93, 128.26, 126.64, 125.44, 123.13, 76.09, 72.53, 30.02, 29.77,

TABLE V: AM1-Calculated Lowest Energy Structures of Phenyl-Substituted TMMs^c

TMM	φ_1^a	φ_1'	φ_2	φ_2'	φ_3	φ_3'	$d_1, \text{\AA}$	$d_2, \text{\AA}$	ϕ_1	ϕ_2	ϕ_3	$\phi_3 + \phi_4 + \phi_5$
	0.0	0.0	0.0	0.0	0.0	0.0	2.635	1.445	146.8	136.2	109.0	359.9
	2.6	1.7	5.2	5.1	4.6	5.7	1.926	1.432	131.6	130.5	108.7	359.9
	23.4	22.1	21.1	20.4	17.9	23.6	2.161	1.430	122.1	123.3	108.7	360.0
	35.9	34.6	12.4	10.9	9.9	13.4	2.232	1.440	121.3	122.6	108.7	360.0
	71.6	72.6	3.9	5.0	5.1	4.8	2.760	1.464	128.4	117.8	108.2	359.9

^a All values of φ (degrees) are reported as deviations from 0° or 180° , whichever was closer. ^b The minimization began from a structure with $\varphi_1, \varphi_2 \sim 73^\circ$. ^c The MM2-minimized structures of the analogous fulvenes were modified to provide the starting structures for the minimization, except where indicated. MOPAC as implemented in InsightII version 2.1.2 (BioSym) was used with the following parameters: triplet state spin-unrestricted, BFGS minimization type, line minimizer off, PRECISE keyword activated, 0.01 kcal/mol convergence criterion. Frequency calculations showed that all structures are true minima; all elements of the diagonalized force constant matrix were positive.

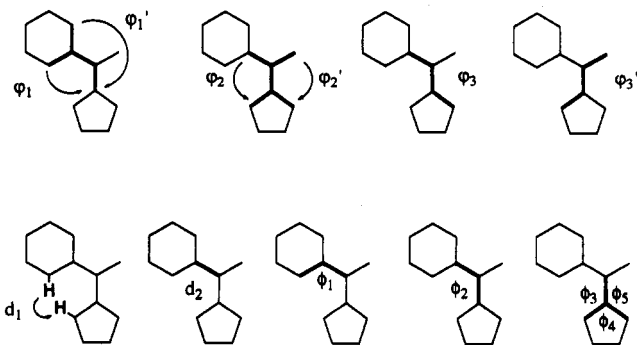
21.49, 21.31. UV λ_{\max} (CH_2Cl_2) 255, 264 (sh), 293, 302, 324, 336, 354 (sh) nm.

Diazene 19(N₂). From 0.301 g of **19r** (0.879 mmol), 850 mg of KOH, and 1.11 g of NiO_x was isolated 139 mg (71%) of a yellow film. ¹H NMR δ 7.15 (m, 4H), 5.72 (d, $\Delta\delta = 2.7$ Hz, 1H), 5.53 (d, $\Delta\delta = 2.7$ Hz, 1H), 2.70 (m, 2H), 2.50 (m, 1H), 2.31 (m, 1H), 1.78 (m, 4H), 1.18 (m, 2H). ¹³C NMR δ 139.10, 138.54, 134.42, 128.40, 127.43, 127.36, 125.38, 125.03, 74.43, 73.80, 29.18, 28.44, 23.27, 21.54, 20.93. UV λ_{\max} (CH_2Cl_2) 249, 288 (sh), 341 (sh) nm.

Diazene 19(N₂)-D₃. This compound was prepared as for **19(N₂)**. ¹H NMR was identical to that of **19(N₂)**, except no multiplets at 2.50 and 2.31 ppm. ¹³C NMR was identical to that of **19(N₂)**, except no singlet at 28.44 ppm. The quintet for the CD₂ carbon was not resolved from baseline noise.

Calculations

Molecular mechanics (MM2)³⁴ and semiempirical (AM1)³⁵ calculations were performed on the fulvenes and TMMs to determine their geometries. Details of the calculations are given in each table heading.



Acknowledgment. We thank the National Science Foundation for support of this work. S.K.S. thanks the NSF for a predoctoral fellowship.

Supplementary Material Available: Full description of X-ray structures of **8** and **9** including atomic coordinates and interatomic distances and angles (23 pages). Ordering information is given on any current masthead page.

References and Notes

- (1) Dedicated to the memory of Gerhard Closs, who taught and inspired us all.
- (2) *Magnetic Molecular Materials*; Gatteschi, D., Kahn, O., Miller, J. S., Palacio, F., Eds.; Kluwer Academic Publishers: Dordrecht, The Netherlands, 1991. *Molecular Crystals and Liquid Crystals*; Miller, J. S., Dougherty, D. A., Eds.; 1989; Vol. 176, pp 1–562. Iwamura, H. *High-Spin Organic Molecules and Spin Alignment in Organic Molecular Assemblies*; Academic Press Ltd.: 1990; Vol. 26, pp 179–253. Dougherty, D. A. *Acc. Chem. Res.* **1991**, *23*, 88–94.
- (3) (a) Dougherty, D. A. *Mol. Cryst. Liq. Cryst.* **1989**, *176*, 25–32. (b) Novak, J. A.; Jain, R.; Dougherty, D. A. *J. Am. Chem. Soc.* **1989**, *111*, 7618–7619. (c) Dougherty, D. A. *Pure Appl. Chem.* **1990**, *62*, 519–524. (e) Kaisaki, D. A.; Chang, W.; Dougherty, D. A. *J. Am. Chem. Soc.* **1991**, *113*, 2764–2766. (f) Dougherty, D. A.; Grubbs, R. H.; Kaisaki, D. A.; Chang, W.; Jacobs, S. J.; Shultz, D. A.; Anderson, K. K.; Jain, R.; Ho, P. T.; Stewart, E. G. In *Magnetic Molecular Materials*; Gatteschi, D., Kahn, O., Miller, J. S., Palacio, F., Eds.; Kluwer Academic Publishers: The Netherlands, 1991; pp 105–120.
- (4) Jacobs, S. J.; Shultz, D. A.; Jain, R.; Novak, J.; Dougherty, D. A. *J. Am. Chem. Soc.* **1993**, *115*, 1744–1753.
- (5) Itoh, K. *Chem. Phys. Lett.* **1967**, *1*, 235–238. Teki, Y.; Takui, T.; Itoh, K. *J. Am. Chem. Soc.* **1983**, *105*, 3722–3723. Sugawara, T.; Bandow, S.; Kimura, K.; Iwamura, H.; Itoh, K. *J. Am. Chem. Soc.* **1986**, *108*, 368–371. Teki, Y.; Takui, T.; Itoh, K.; Iwamura, H.; Kobayashi, K. *J. Am. Chem. Soc.* **1986**, *108*, 2147–2156. Nakamura, N.; Inoue, K.; Iwamura, H. *J. Am. Chem. Soc.* **1992**, *114*, 1484–1485. Wright, B. B.; Platz, M. S. *J. Am. Chem. Soc.* **1983**, *105*, 628–630.
- (6) See, for example: Kato, S.; Morokuma, K.; Feller, D.; Davidson, E. R.; Borden, W. T. *J. Am. Chem. Soc.* **1983**, *105*, 1791–1795 and references therein.
- (7) (a) Dowd, P. *J. Am. Chem. Soc.* **1966**, *88*, 2587–2589. (b) Dowd, P. *Acc. Chem. Res.* **1972**, *5*, 242–248. (c) Berson, J. A. In *Diradicals*; Borden, W. T., Ed.; John Wiley and Sons: New York, 1982; pp 151–194.
- (8) Dvolaitzky, M.; Chiarelli, R.; Rassat, A. *Angew. Chem. Int. Ed. Engl.* **1992**, *31*, 180–181.
- (9) Kanno, F.; Inoue, K.; Koga, N.; Iwamura, H. *J. Am. Chem. Soc.* **1993**, *115*, 847–850.
- (10) Rajca, A.; Utamapanya, S. *J. Am. Chem. Soc.* **1993**, *115*, 2396–2401 and references therein.

(11) See, for example: Dougherty, D. A. In *Kinetics and Spectroscopy of Carbenes and Biradicals*; Platz, M. S., Ed.; Plenum Press: New York, 1990; pp 117-142.

(12) We have prepared several other derivatives of 4 in which the benzene ring is replaced by a pyridine, a phenol, or a phenoxide. In all cases, behavior similar to that seen for 4 is displayed. Silverman, S. K., unpublished results.

(13) TMMs of the present type are completely stable to the photolysis conditions,⁴ so photodestruction of the molecule is not a viable explanation.

(14) Carilla, J.; Juliá, L.; Riera, J.; Brillas, E.; Garrido, J. A.; Labarata, A.; Alcalá, R. *J. Am. Chem. Soc.* **1991**, *113*, 8281-8284. See also: Ling, C.; Lahti, P. M. *Chem. Lett.* **1993**, 769-772.

(15) Kollmar, H.; Staemmler, V. *Theor. Chim. Acta* **1978**, *48*, 223-239. Borden, W. T. In *Diradicals*; Borden, W. T., Ed.; John Wiley & Sons: New York, 1982; pp 1-72. Brooks, B. R.; Schaefer, H. F., III. *J. Am. Chem. Soc.* **1979**, *101*, 307-311. Buenker, R. J.; Peyerimhoff, S. D. *Chem. Phys.* **1975**, *9*, 75-89.

(16) Carrington, A.; Smith, I. C. P. *Mol. Phys.* **1969**, *9*, 137-147.

(17) Fulvene (λ_{\max} (nm) in CH_2Cl_2): **11f** (267), **10f** (300), **19f** (324), **18f** (345), **17f** (341, with extensive fine structure).

(18) All $\Delta m_s = 2$ hyperfine couplings are well simulated by a binomial distribution of Gaussian peaks. This is a valid procedure for systems with small D values. See, for example: Jain, R.; Sponsler, M. B.; Coms, F. D.; Dougherty, D. A. *J. Am. Chem. Soc.* **1988**, *110*, 1356-1366.

(19) Jain, R.; McElwee-White, L.; Dougherty, D. A. *J. Am. Chem. Soc.* **1988**, *110*, 552-560.

(20) Sponsler, M. B.; Jain, R.; Coms, F. D.; Dougherty, D. A. *J. Am. Chem. Soc.* **1989**, *111*, 2240-2252.

(21) (a) Conradi, M. S.; Zeldes, H.; Livingston, R. J. *Phys. Chem.* **1979**, *83*, 633-637. (b) Berson, J. A.; Griller, D.; Owens, K.; Wayner, D. D. M. *J. Org. Chem.* **1987**, *52*, 3316-3319.

(22) The temperatures over which the changes in Figure 10 occur seem consistent with other examples of hindered methyl rotation.^{23,24}

(23) Wiberg, K. B.; Martin, E. *J. Am. Chem. Soc.* **1985**, *107*, 5035-5041.

(24) Clough, S.; Poldy, F. *J. Chem. Phys.* **1969**, *51*, 2076-2084. Fessenden, R. W.; Schuler, R. H. *J. Chem. Phys.* **1963**, *39*, 2147-2195.

(25) The diphenyl derivative of 3 shows considerable variation in the zfs E parameter.^{7c}

(26) Stille, J. R.; Grubbs, R. H. *J. Org. Chem.* **1989**, *54*, 434-444.

(27) Weiberth, F. J.; Hall, S. S. *J. Org. Chem.* **1987**, *52*, 3901-3904.

(28) Sardella, D. J.; Keane, C. M.; Lemonias, P. *J. Am. Chem. Soc.* **1984**, *106*, 4962-4966.

(29) Tsatsas, G.; Cotakis, G. *Bull. Soc. Chim. Fr.* **1970**, 3609-3616.

(30) Logullo, F. M.; Seitz, A. H.; Friedman, L. *Org. Synth. Coll. Vol. V* **1973**, 54-59.

(31) Abou-Teim, O.; Goodland, M. C.; McOmie, J. F. W. *J. Chem. Soc., Perkin Trans. I* **1983**, 2659-2662.

(32) Stone, K. J.; Little, R. D. *J. Org. Chem.* **1984**, *49*, 1849-1853.

(33) Gatto, K.; Reinheimer, J. P.; Shafer, K. *Org. Magn. Res.* **1974**, *6*, 577-579.

(34) Allinger, N. L. *J. Am. Chem. Soc.* **1977**, *99*, 8127-8134. Burkert, U.; Allinger, N. L. *Molecular Mechanics*; ACS Monograph 177; American Chemical Society: Washington, DC, 1982.

(35) Dewar, M. J. S.; Thiel, W. *J. Am. Chem. Soc.* **1985**, *107*, 3902.